ARTICLE TYPE
www. rsc.org/xxxxxx | XXXXXXXX

Acoustofluidic control of bubble size in microfluidic flow-focusing configuration†

Zhuang Zhi Chong,[a] Shu Beng Tor,[a] Ngiap Hiang Loh,[a] Teck Neng Wong,[a] Alfonso M Gañán-Calvo,[b] Say Hwa Tan,*[a] Nam-Trung Nguyen,*[c]

Received Xth XXXXXXXXXX 20XX, Accepted Xth XXXXXXXXX 20XX
First published on the web Xth XXXXXXXXXX 20XX **DOI: 10.1039/b000000x**

This paper reports a method to control the bubble size generated in a microfluidic flow-focusing configuration. With an ultrasonic transducer, we induce acoustic streaming using a forward moving, oscillating gas-liquid interface. The induced streaming substantially affect the formation process of gas bubbles. The oscillating interface acts as a pump that increases the gas flow rate significantly and forms a larger bubble. This method is applicable to wide range of gas pressure from 30 to 90 kPa and flow rate from 380 to 2700 μL/h. The bubble size can be tuned repeatably with a response time in the order of seconds. We believe that this method will enhance the capability of a microfluidic bubble generator to produce tunable bubble size.

1 Introduction

Micrometer size bubbles are used in numerous applications such as ultrasonic scanning, drug discovery and two phase micromixing.[1] Microfluidic devices of different designs including flow-focusing, T-junction and co-flowing configurations have been used to generate monodisperse microbubbles.[2]

In this work, we use a microfluidic flow-focusing device. Droplet generation using this kind of device enjoys a wide range of methods to control the formation process of micro droplets and their size: common active methods are based on acoustic[3], electric,[4] and thermal.[5] The main reasons for this multiplicity of possibilities in droplet generation come from two fundamental facts: (i) the densities of both disperse and carrier phases are similar, and (ii) surface tension between two liquids is often very small. Thus, any physical action fundamentally associated to the presence of the interface will efficiently affect both phases.

However, bubble generation involves two phases, one of which has a negligible density compared to the other, and surface tension between both is generally much larger than in liquid-liquid pairs. This, conversely, has two dramatic consequences: (i) externally induced interfacial effects are generally masked by a large surface tension, and (ii) interfacial actions fundamentally affect the liquid phase only (except in limited regions of the fluid domains). Therefore, the control of the bubble size using these devices is limited by a few parameters such as the flow rate, applied pressure and the geometry of the channel.[6]

From the applications standpoint, there is a need to address this capability gap between bubble generation and droplet generation, which opens a very valuable niche for ingenuity. On the quest for a better control, some ideas to profitably focus some excess energy on the interface in similar configurations to enhance surface generation (i.e. a dramatic decrease in bubble diameter under the same flow rates and applied pressures) have been recently proposed, including swirl[7] or the use of patterned surfaces.[8] However, these proposals imply design and fabrication challenges that the microfluidic flow-focusing lack. In this work, we report a serendipitous way not only to achieve a remarkable control on the bubble size in microfluidic flow-focusing, but also to gain a nearly global immediate response from the system (something out of the reach of most microfluidic systems): we mechanically activate the system, and inextricably, the interface, by ultrasonic excitation, to provoke immediate changes in the flow pattern and the bubbles generated.

Bubbles expand and contract with the acoustic pressure rarefaction and compression.[9] Driven by an acoustic pressure, bubbles rectify the rapid oscillation motion of the gas-liquid interface into steady streaming flow in the liquid around the bubbles.[10] This Rayleigh type of acoustic streaming is different than quartz wind streaming that operates in the MHz range.[11] The streaming flow has been used in microfluidic devices for mixing,[12] pumping,[13] sorting of microparticles[14] and sonoporation of suspended cells.[15]

The bubbles that induces Rayleigh streaming in microfluidic devices are typically formed by passing liquids along

[a] *School of Mechanical and Aerospace Engineering, Nanyang Technological University, 50 Nanyang Avenue, Singapore 639798. Email: sayhwa.tan@gmail.com*
[b] *Depto. de Ingeniería Aeroespacial y Mecánica de Fluidos, Universidad de Sevilla, E-41092 Sevilla, Spain.*
[c] *QLD Micro- and Nanotechnology Centre, Nathan campus, Griffith University, 170 Kessels Road QLD 4111, Australia. Email: nam-trung.nguyen@griffith.edu.au*
† Electronic Supplementary Information (ESI) available.

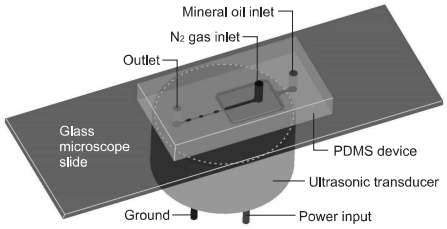

Fig. 1 Bubble generation device with ultrasonic transducer. The schematic is not drawn to the scale.

blind side channels filled with gas.[12] These trapped semicylindrical air bubbles are difficult to form with a desired size as suitable wetting properties, blind side channels geometry, and initial flow conditions are required. Furthermore, the bubble size will change after a period of continuous oscillation. Once the device has failed to create or maintain a bubble with desired size, it will need to be replaced.

Instead of trapping bubbles in blind side channels with challenging repeatability, our setup induces streaming using a forward moving gas-liquid interface during bubble generation process. The induced streaming alters the behavior of bubble formation and thus its generated bubble size. This offers a new and novel way to control the generated bubble size while maintaining the fluid flow rate or pressure.

2 Materials and methods

The polydimethylsiloxane (PDMS) device with a cross-junction design (width w of 100 μm and height h of 43 μm) was fabricated using standard soft lithography techniques.[16] The bottom part of the device was coated with a thin layer of ultrasound gel (ZG-F, General Electric) before being attached to an ultrasonic transducer (328ET250, Prowave), Fig. 1. The transducer was positioned so that its center aligns with the center of the cross-junction of the microchannels. When the transducer is not properly centered, the induced streaming reduces significantly which in turn results in a smaller increase in the size of the bubbles produced.

We form bubbles in oil by flowing nitrogen gas to the central channel of the cross junction and mineral oil (M5904, Sigma Aldrich; viscosity η = 30 mPa s; surface tension σ = 33 mN/m) to the two side channels. The hydrophobic wetting nature of the PDMS material only allows stable formation of bubbles in oil for our case. A syringe pump (neMESYS, Cetoni) provides a constant volumetric flow rate of the oil while a pressure controller (PPC4, Fluke) maintains the pressure of the gas. We capture the bubble generation using a microscope (BX51, Olympus) fitted with a high-speed camera (Miro M310, Phantom). The bubble dimensions and generation frequency were evaluated from recorded videos using a customized image processing software based on the OpenCV platform.

An alternating current (AC) source supplies the power to the transducer. The source is produced by amplifying a sinusoidal voltage from a signal generator (33520A, Agilent) using an operational amplifier (OPA552, Texas Instruments). AC frequency up to 400 kHz and a peak-to-peak voltage up to 40 V were used in our experiment. As the transducer heats up during the operation, a fan (MCF-J01BM05-9, Toshiba) provides convective cooling to prevent the temperature at the junction from increasing more than 2°C in 10 minutes. The temperature is measured by inserting a Type K thermocouple into the microfluidic device. The transducer is switched off immediately after each data acquisition to prevent overheating.

3 Results and discussion

Monodisperse bubbles were formed under a gas pressure of 45 kPa and an oil flow rate of 960 μL/h. Subsequently, the size of generated bubbles was investigated under a frequency search from 1-400 kHz with 1 kHz interval. The bubbles showed a significant increase in size when the actuation frequency is tuned to 128 kHz and 290 kHz. Fig. 2(a) shows the frequency response of the bubble size in the range of 120 to 136 kHz, which has a sharp peak at 128 kHz.

Keeping the actuation condition at 40 V and 128 kHz, the process of the bubble generation was captured by a high-speed camera at a rate of 192,440 frames per second. Video01.mp4[†] shows an oscillatory motion of gas-liquid interface. The speed of the motion is much faster than the forward movement of the gas-liquid interface. The interface oscillates in the principal, volumetric mode as no nodes were observed at the moving interface and the large channel provides the necessary gas source for the volumetric oscillation.

We believe that 128 kHz is not the resonant frequency of the gas-liquid interface. Firstly, resonant frequency of the gas-liquid interface depends on its radius of curvature and the fluidic pressure, as indicated in the solution from Rayleigh-Plesset equation.[17] The resonant frequency changes as the radius of the gas-liquid interface curvature continuously changes throughout the bubble generation process. If the interface is oscillating at a resonant frequency, vigorous motion can only be observed for a short period. However, the video shows that the interface oscillates with the same amplitude throughout the whole process. Furthermore, the frequency would increase when the oil flow rate and gas pressure increases. Yet, experimental results showed that 128 kHz is still the frequency that produces the maximum bubble size over a range of oil flow rate and the gas pressure up to 2700 μL/h and 90 kPa, respectively.

We hypothesise that the optimal frequency is the mechanical vibration mode of the transducer system. This hypothe-

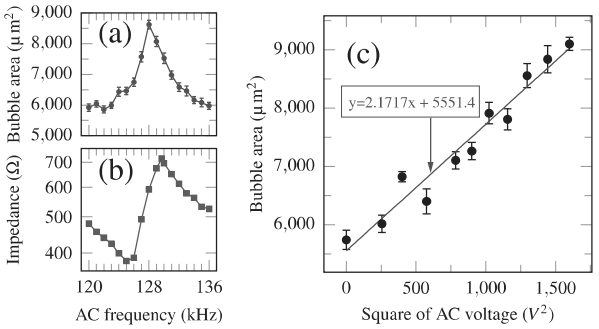

Fig. 2 Tuning bubble size using actuation frequency and magnitude: (a) Frequency spectrum of bubble size; (b) Electrical impedance of the transducer over the same range of frequency (120–136 kHz); (c) Bubble size versus applied voltages at 128 kHz. The flow condition of bubble generation in (a-c) is $P = 45\ kPa$, $Q_l = 960\ \mu L/h$.

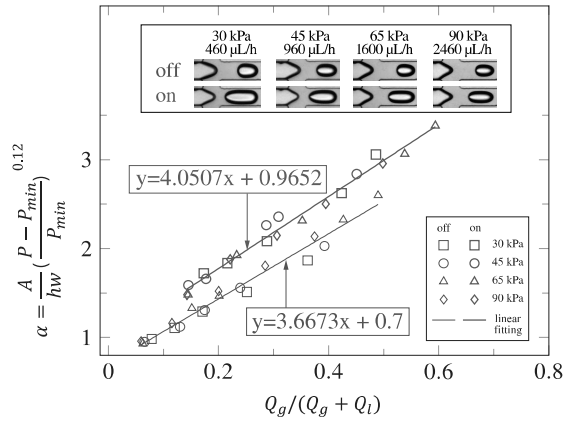

Fig. 3 Generated bubble size in dimensionless number under different flow conditions with and without actuation. The insets show the generated bubbles under the selected flow condition.

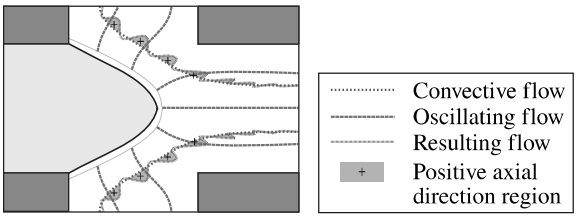

Fig. 4 Generic streaming pathlines resulting from the combination of convective and oscillating flow.

sis was tested by measuring the electrical impedance of the transducer system, as a pair of electrical resonance and antiresonance (local minimum and maximum impedance magnitude) is usually found around the mechanical resonance of piezoelectric actuators.[18] The measurement on the attached transducer showed that this pair of electrical resonance does exist around 128 kHz, Fig. 2(b). Another pair around 290 kHz was also identified, which we also observed a significant increase in bubble size, yet smaller effect than the one at 128 kHz. Therefore, although the effect of acoustic wave resonances along the gas feeding channel cannot be completely ruled out, we can conclude that the vibration modes of the transducer system controls the increase in bubble size. The electrical impedance measurements of the transducer can be found in Fig. S1†.

In a subsequent test, we monitor the size of the bubble generated under the same flow condition with varying applied voltage at a fixed frequency of 128 kHz. Fig. 2(c) shows that bubble area is a square function of of the applied AC voltage. Thus the increase in bubble area is proportional to the energy input through the transducer.

We then evaluated the role of pressure and flow rate at a fixed actuation condition of 40 V, 128 kHz. For all the tested flowing conditions, the size of the generated bubble was found to increases significantly after turning on the transducer, as plotted in Fig. S2†. The insets in Fig. 3 shows the generated bubbles under different flow conditions with and without actuation. The evaluation is also shown using the contours tracing of the expansion process of the gas-liquid interface under various flow conditions (Fig. S3†). In all the tested condition, the interface expands upon the activation of transducer.

The result is plotted in Fig. 3 using dimensionless numbers which the relationship[19] is indicated in the x and y-axis labels. The α, Q_g, and Q_l are dimensionless bubble area, gas volumetric flow rate and liquid volumetric flow rate respectively. The variable α was determined using bubble area A, gas pressure P, channel height h and channel width w. The second term in the derivation of α is a small correction factor for pressure, where P_{min} is the minimum pressure (20 kPa) to achieve stable bubble formation and 0.12 is the fitting power for the relationship. Gas flow rate, Q_g was calculated from the generation frequency and the average volume of a bubble. The volume of a bubble is estimated using the equation mentioned by van Steijn et al.[20] Fig. 3 shows that the gas flow rate increases when transducer is turned on. The alpha values converges to a line above the line without actuation following a similar gradient.

The increase in size of generated bubbles upon the activation of the transducer can be related to the Rayleigh streaming formed around the gas-liquid interface. This streaming is induced by the rapid oscillation of the interface,[10] with $u_s \sim 2\pi f \varepsilon^2 a$ as the theoretical streaming velocity.[14] At $Q_l = 960\ \mu L/h$ and $P = 45\ kPa$, the theoretical streaming velocity is ~26 mm/s ($\varepsilon = 0.04$, $a = 20\ \mu m$, $f = 128\ kHz$, where εa is the oscillation amplitude and a is the radius of curvature). This order of magnitude is comparable to the average oil flow velocity of 62 mm/s.

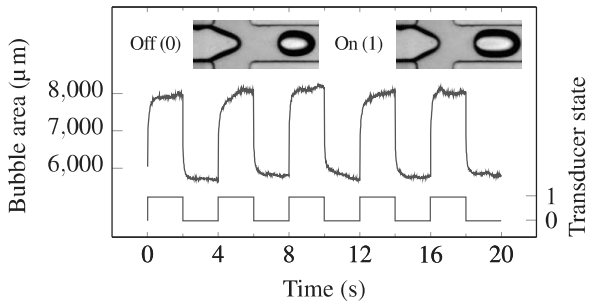

Fig. 5 Generated bubble size response to the transducer state. Insets shows the images from capturing at off (0) state and on (1) state.

In order to explain the mechanism, we propose possible pathlines of the streaming interaction as illustrated in Fig. 4 based on detailed observation on the experimental results. The pathlines are the resulting flow between the convective and oscillating flow. The resulting flow pathlines deviate from the convective ones with a net difference in the positive axial direction. This difference promotes a net pumping effect that increases the flow rate of gas and thus increases the generated bubble size.

We will also like to highlight that the streaming path lines formed around the forward moving oscillating gas-liquid interface in a fast flowing medium is a complex problem by itself in nature. A detailed numerical simulation is currently in progress to study specifically the path lines due to the interaction. However, our current proposed model is a reasonable hypothesis which justifies the obtained experimental results. The velocity of the induced streaming around the oscillating interface is in the order comparable to the flow velocity.

Next, repeatability test was carried out for a constant flow condition ($P = 45$ kPa, Q_l=960 μL/h). In this test, the transducer is switched on and off every two seconds. Fig. 5 shows the test results, where 1 and 0 are on and off state of the transducer, respectively. The size response of the formed bubble to the transducer state is repeatable. The data show a sharp rise or fall in the bubble area around the switching points. The change in bubble size within 100 ms is shown in Video02.mp4[†]. This observation indicates that the induced streaming is formed very quickly after turning on the transducer.

4 Conclusions

We demonstrated a method to control the generated bubble size in flow-focusing configuration using an ultrasonic transducer. We induced acoustic streaming using a forward moving, oscillating gas-liquid interface at the resonance mode of the transducer system. The induced streaming clearly affected the process of bubble formation. The gas flow rate and generated bubble size increased significantly when the transducer is turned on. This method was applied and had the same effect to variable flow conditions such as gas pressure ranging from 30 to 90 kPa, and flow rate ranging from 380 to 2700 μL/h. The range of the generated bubble size changes from 3543-10133 μm^2 without transducer to 5474-14285 μm^2 when excited by transducer. The increase in the generated bubble size was repeatable in seconds. This method is a low-cost and simple way to enhance the capability of microfludic bubble generator to produce a wide range of bubble size with a possible feedback control.

Acknowledgments

S.H. Tan & T.N. Wong gratefully acknowledge the research support from the Singapore Ministry of Education (MOE) Tier 2 Grant (No. 2011-T2-1-0-36). We also gratefully acknowledge insightful discussion with Prof Claus-Dieter Ohl at Nanyang Technological University, Singapore.

References

1 N. Dietrich, S. Poncin, N. Midoux and H. Z. Li, *Langmuir : the ACS journal of surfaces and colloids*, 2008, **24**, 13904–11.
2 T. Fu, D. Funfschilling, Y. Ma and H. Z. Li, *Microfluidics and Nanofluidics*, 2009, **8**, 467–475.
3 L. Schmid and T. Franke, *Lab on a chip*, 2013, **13**, 1691–4.
4 S. H. Tan, B. Semin and J.-C. Baret, *Lab on a Chip*, 2014.
5 S. H. Tan, S. M. Sohel Murshed, N.-T. Nguyen, T. N. Wong and L. Yobas, *Journal of Physics D: Applied Physics*, 2008, **41**, 165501.
6 S.-K. Hsiung, C.-T. Chen and G.-B. Lee, *Journal of Micromechanics and Microengineering*, 2006, **16**, 2403–2410.
7 M. A. Herrada and A. M. Gañán Calvo, *Physics of Fluids*, 2009, **21**, 042003.
8 M. A. Herrada, A. M. Gañán Calvo and J. M. Montanero, *Physical Review E*, 2013, **88**, 033027.
9 K. Ferrara, R. Pollard and M. Borden, *Annual review of biomedical engineering*, 2007, **9**, 415–47.
10 C. Wang, S. V. Jalikop and S. Hilgenfeldt, *Biomicrofluidics*, 2012, **6**, 12801–1280111.
11 N. T. Nguyen and R. M. White, *IEEE transactions on ultrasonics, ferroelectrics, and frequency control*, 2000, **47**, 1463–71.
12 D. Ahmed, X. Mao, B. K. Juluri and T. J. Huang, *Microfluidics and Nanofluidics*, 2009, **7**, 727–731.
13 A. R. Tovar and A. P. Lee, *Lab on a chip*, 2009, **9**, 41–3.
14 C. Wang, S. V. Jalikop and S. Hilgenfeldt, *Applied Physics Letters*, 2011, **99**, 034101.
15 S. L. Gac, E. Zwaan, A. van den Berg and C.-D. Ohl, *Lab on a chip*, 2007, **7**, 1666–72.
16 D. C. Duffy, J. C. McDonald, O. J. Schueller and G. M. Whitesides, *Analytical chemistry*, 1998, **70**, 4974–84.
17 T. Leighton, *The acoustic bubble*, Academic Press, San Diego London, 1994.
18 J. Pons, *Emerging Actuator Technologies*, John Wiley & Sons, Ltd, Chichester, UK, 2005.
19 T. Cubaud, M. Tatineni, X. Zhong and C.-M. Ho, *Physical Review E*, 2005, **72**, 037302.
20 V. van Steijn, C. R. Kleijn and M. T. Kreutzer, *Lab on a chip*, 2010, **10**, 2513–8.